

## Articles

## Site-Selective Self-assembly of MPA-Bridged CuHCF Multilayers on APTMS-Supported Gold Colloid Electrodes

Wenlong Cheng, Shaojun Dong, and Erkang Wang\*

State Key Laboratory of Electroanalytical Chemistry, Changchun Institute of Applied Chemistry, Chinese Academy of Sciences, Changchun, Jilin 130022, People's Republic of China

Received October 24, 2002. Revised Manuscript Received January 7, 2003

(3-Aminopropyl)trimethoxysilane (APTMS)-supported gold colloid electrode was constructed by virtue of a recently developed solution-based self-assembly strategy. The preparing procedure of 3-mercaptopropionic acid (MPA)-bridged copper hexacyanoferrate (CuHCF) multilayers on a planar macroelectrode (Bharathi et al. *Langmuir* **2001**, *17*, 7468) was copied to the as-prepared colloid electrode. The optical spectra, atomic force microscopy, and electrochemistry demonstrate successful copy of the multilayer system on a macroelectrode to the as-prepared colloid electrode. Remarkably, it was found that multilayer growth is highly selective to the nanoscale sites where gold nanoparticles are immobilized, and multilayer growth does not take place on the sites without nanoparticles. Interestingly, a preliminary electrochemical investigation indicates that electrochemical properties of multilayers systems on the colloid electrode are different from their counterparts on a planar macroelectrode, which might be due to high curvature effects of the gold nanoparticles. This indicates a different motif of multilayers on the colloid electrode from that on a planar macroelectrode.

### Introduction

Recently, a solution-based strategy was developed for preparing SERS and SPR substrates,<sup>1</sup> which are fabricated by constructing an adhesive molecular layer on a conductive support and subsequent adsorption of metal nanoparticles on the adhesive layer. These molecularly linked nanoparticle films were demonstrated to behave as a bulk macroelectrode and exhibited potential electrochemical applications.<sup>2</sup> Therefore, these nanoparticle films are called colloid electrodes in this text for clarity. The colloid electrode consists of incontinuously distributed high-area-ratio nanoparticles, which result in high electrochemical responses of redox-active thiolate monolayers.<sup>3</sup> The colloid electrode was also demonstrated to be able to act as base substrates for photopolymerizable self-assembled monolayers.<sup>4</sup> We observed more revers-

ible redox electrochemistry of  $\text{AsMoVO}_{40}^{4-}$  anions on the colloid electrode than that on a planar macroelectrode,<sup>2d</sup> which shows nanoscale surface geometry affects molecular adsorptive and interactions, especially, when adsorptive molecules have dimensions comparable to those of nanoparticles. Weaver and co-workers<sup>5</sup> prepared the gold colloid electrodes modified with uniform Pt-group overlayers by using copper UPD on the colloid electrode and subsequent immersion in the salts of the Pt group. The epitaxial Pt-group layers can be controlled to the monolayer level, which indicates the broader possibility of utilizing immobilized gold nanoparticle templates to prepare nanomaterials having widely varying size, structure, chemical constituents, and novel properties.

As an extension of these previous reports on monolayer-level surface modification of these immobilized nanoparticles,<sup>2–5</sup> this study is aimed at demonstrating feasibility of anchoring some multilayer systems to the colloid electrode. Self-assembled multilayer systems were widely studied due to their potential applications in molecular electronics as many complicated structures can be assembled with molecular precision.<sup>6</sup> Multilayers formed by ionic interactions are of interest as they are easy to prepare and have good stability.<sup>7</sup> For example, such multilayers by virtue of ionic interactions were

\* To whom correspondence should be addressed. E-mail: ekwang@ciac.jl.cn. Fax: +86-431-5689711.

(1) (a) Freeman, R. G.; Grabar, K. C.; Allison, K. J.; Bright, R. M.; Davis, J. A.; Guthrie, A. P.; Hommer, M. B.; Jackson, M. A.; Smith, P. C.; Walter, D. G.; Natan, M. J. *Science* **1995**, *267*, 1629. (b) Grabar, K. C.; Smith, P. C.; Musick, M. D.; Davis, J. A.; Walter, D. G.; Jackson, M. A.; Guthrie, A. P.; Natan, M. J. *J. Am. Chem. Soc.* **1996**, *118*, 1148.

(2) (a) Cheng, W. L.; Dong, S. J.; Wang, E. *Anal. Chem.* **2002**, *74*, 3599. (b) Cheng, W. L.; Dong, S. J.; Wang, E. *Langmuir* **2002**, *18*, 9947. (c) Cheng, W.; Jiang, J. G.; Dong, S. J.; Wang, E. *Chem. Commun.* **2002**, *1706*. (d) Cheng, W. L.; Dong, S. J.; Wang, E. Unpublished results.

(3) Doron, A.; Katz, E.; Willner, I. *Langmuir* **1995**, *11*, 1313.

(4) Menzel, H.; Mowery, M. D.; Cai, M.; Evans, C. E. *Adv. Mater.* **1999**, *11*, 131.

(5) Park, S.; Yang, P.; Corredor, P.; Weaver, M. J. *J. Am. Chem. Soc.* **2002**, *124*, 2428.

artfully used as molecular rulers<sup>8</sup> to scale down predetermined patterned gold surfaces. This indicates feasibility of anchoring ionic reactive multilayers to gold nanostructures. We reasoned that such selective growth could also take place on the nanostructured gold colloid electrode. For a convenient characterization, a recently developed 3-mercaptopropionic acid (MPA)-bridged copper hexacyanoferrate (CuHCF) multilayers system developed by Ikeda and co-workers<sup>9</sup> is selected because such multilayers are highly stable, reproducible, and electrochemically addressable. As a result, selective deposition of CuHCF multilayers on a gold colloid electrode was achieved, which was demonstrated by UV-vis spectroscopy, tapping-mode atomic force microscopy (AFM), and cyclic voltammograms. Further electrochemical studies show larger deviation from ideal surface-bound redox electrochemistry than that in ref 9, which might be due to high-curvature effects of gold nanoparticles.

## Experimental Section

**Materials.** HAuCl<sub>4</sub>·3H<sub>2</sub>O, Cu(NO<sub>3</sub>)<sub>2</sub>, trisodium citrate, (3-aminopropyl)trimethoxysilane (APTMS), MPA, and potassium ferricyanide were obtained from Aldrich and used as received. All other reagents were of analytical grade and were used also without further purification. Pure water was obtained by passing it through a Millipore Milli-Q water purification system. Its resistivity is over 18 MΩ·cm. Indium-doped tin oxide (ITO) glass was purchased from Changchun Institute of Optics and Mechanics with a sheet resistance of 80 Ω cm<sup>-2</sup>.

**Preparation of Gold Colloids.** All glasswares used in the following procedures were cleaned in a bath of freshly prepared 3:1 HCl:HNO<sub>3</sub> and rinsed thoroughly in H<sub>2</sub>O prior to use. The gold colloids were prepared by the conventional citrate reduction of HAuCl<sub>4</sub> in water at near-boiling temperature.<sup>2,10</sup>

**Instruments.** Electrochemical experiments were carried out on an Autolab PGSTAT30 potentiostat (Utrecht, The Netherlands) in a conventional one-compartment cell. The cell<sup>10</sup> was housed in a homemade Faraday cage to reduce stray electrical noise. All measurements were done using standard three-electrode systems. A Ag/AgCl electrode was used as the reference electrode and Pt foil as the counter electrode and the O-ring with 6-mm inner diameter was used to seal the ITO electrode for all electrochemical experiments (geometrical area is ca. 0.283 cm<sup>2</sup>). Optical spectra were acquired using a Cary 500 UV-visible NTR spectrometer (Varian, USA). AFM images were taken by using a Nanoscope IIIa instrument operating in the tapping mode with standard silicon nitride tips. Typically, the surface was scanned at 1 Hz with 256 lines per image resolution and a 1.0–3.0 V setpoint.

**Preparation of the Gold Colloid Electrode and Self-assembly of MPA-Bridged CuHCF Multilayers on It.** The ITO substrate was ultrasonicated for 20 min in each of the following solvents: soapy water, water, acetone, and methanol. After thorough cleaning, the ITO substrate was immersed in

2% (v:v) APTMS methanol solution for 1 day. After exhaustive rinsing by methanol, the APTMS-derivatized substrate was then immersed in the as-prepared Au colloid (~6 nM) for 50 min, rinsed thoroughly by water, and stored in water before use. The surface morphologies of the as-prepared colloid electrodes were evaluated by AFM, and simple particle number counting in AFM images with unit area can determine nanoparticle surface coverage. The colloid electrode with ~10% surface coverage of gold nanoparticles was used purposively for AFM studies.

The overall preparative process of CuHCF multilayers on the gold colloid electrode is shown in Scheme 1. The first step depicts APTMS anchoring on the ITO surface. The second step illustrates linkage of the gold nanoparticle to the ITO via an amino moiety of the polymerized APTMS adhesive layer. Subsequent modification of the colloid layer includes three consecutive steps: (3) immersion into 10 mM methanolic solution of MPA for about 20–30 min; (4) dipping into a 10 mM Cu(NO<sub>3</sub>)<sub>2</sub> solution for 20 min, which leads to the formation of a monolayer of Cu<sup>2+</sup>-carboxylate complex surrounding nanoparticles;<sup>7,9</sup> (5) dipping into 10 mM potassium ferricyanide solution for 20 min, which results in the formation of a CuHCF monolayer surrounding nanoparticle. Repetition of these three steps (3, 4, 5 in Scheme 1) on CuHCF monolayer leads to the formation of CuHCF multilayers centered on individual immobilized gold nanoparticles. The mechanism for the formation of MPA-bridged CuHCF multilayers on a planar macroelectrode has been described previously.<sup>9</sup> The primary driving forces for multilayer formation are interactions between the copper ions with carboxylate of MPA and interactions between Cu<sup>2+</sup> present in the CuHCF and thiol groups of MPA.<sup>7,9</sup>

## Results and Discussion

**Evidence of Selective Anchoring of CuHCF Multilayers on the Nanoscale Domains Where Gold Nanoparticles Are Immobilized.** It is known that metal nanoparticles such as Au, Ag, and Cu possess strong absorption in the visible region, often coined as surface plasmon absorption. Such resonance occurs when the incident photon frequencies match the collective oscillations of the conduction electrons of metal nanoparticles. The optical and electronic properties of these metal nanoparticles are dependent on the surrounding environment,<sup>11</sup> particle size, and shape.<sup>12</sup> These characteristic properties are also exhibited when these nanoparticles are tethered to a solid substrate (that is, the colloid electrode or these nanoparticle films still have a characteristic plasmon absorption band). The plasmon band is highly sensitive to the surrounding environment and was demonstrated to behave as a sensitive nanoscale optical biosensor.<sup>13</sup> When foreign species adsorb on these immobilized nanoparticle sur-

(6) (a) Finklea, H. O. In *Electroanalytical Chemistry*, Bard, A. J., Rubinstein, I., Eds.; Marcel Dekker: New York, 1996; Vol. 19, pp 109–1335. (b) Allara, D. L.; Dunbar, T. D.; Weiss, P. S.; Bumm, L. A.; Cygan, M. T.; Tour, J. M.; Reinerth, W. A.; Yao, Y.; Kozaki, M.; Jones, L. *Ann. N. Y. Acad. Sci. (Mol. Electron.: Sci. Technol.)* **1998**, 852, 349.

(7) (a) Lee, H.; Kepley, L. J.; Hong, H.-G.; Mallouk, T. E. *J. Am. Chem. Soc.* **1988**, 110, 618. (b) Li, D.; Ratner, M. A.; Marks, T. J. *J. Am. Chem. Soc.* **1990**, 112, 1430. (c) Brust, M.; Blass, P. M.; Bard, A. J. *Langmuir* **1997**, 13, 5602. (d) Hatzor, A.; Van der Boom-Moav, T.; Yochelis, S.; Vaskevich, A.; Shanzer, A.; Rubinstein, I. *Langmuir* **2000**, 16, 4420.

(8) Hatzor, A.; Weiss, P. S. *Science* **2001**, 291, 1019.

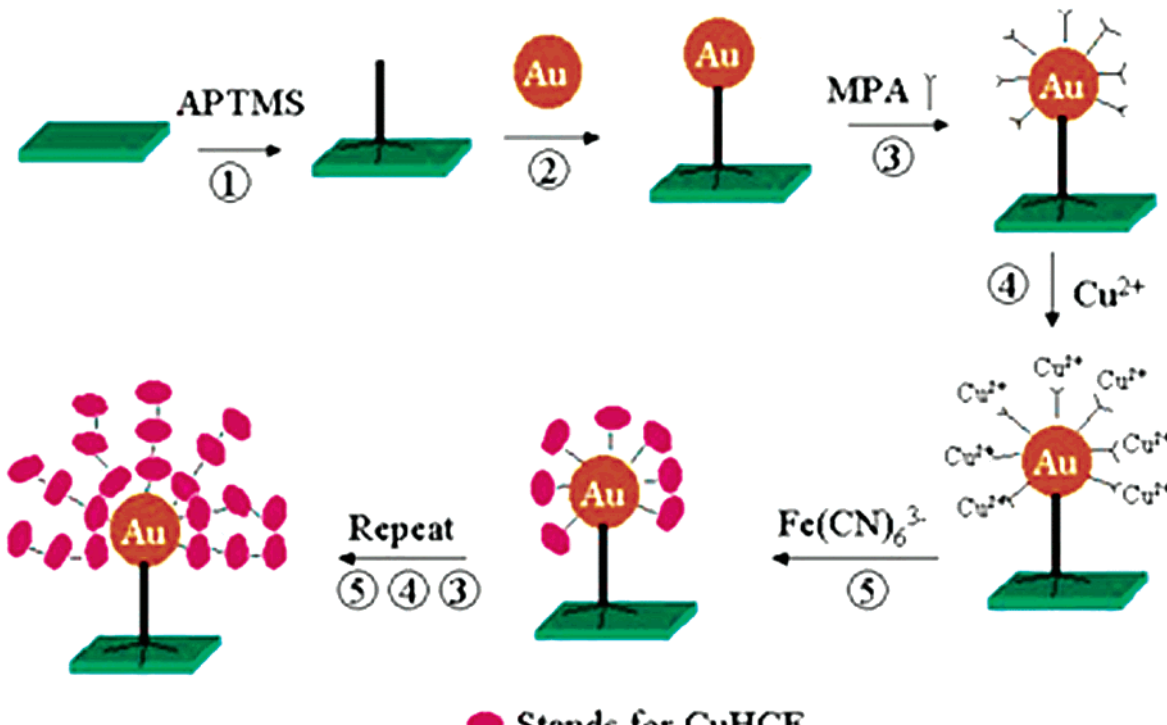
(9) Bharathi, S.; Nogami, M.; Ikeda, S. *Langmuir* **2001**, 17, 7468.

(10) (a) Frens, G. *Nature Phys. Sci.* **1973**, 241, 20. (b) Grabar, K. C.; Freeman, R. G.; Hommer, M. B.; Natan, M. J. *Anal. Chem.* **1995**, 67, 735.

(11) (a) Kreibig, U.; Volmer, M. *Optical Properties of Metal Clusters*; Springer-Verlag: Heidelberg, Germany, 1995. (b) Eck, D.; Helm, C. A.; Wagner, N. J.; Vaynberg, K. A. *Langmuir* **2001**, 17, 957. (c) Templeton, A. C.; Pietron, J. J.; Murray, R. W.; Mulvaney, P. *J. Phys. Chem. B* **2000**, 104, 564. (d) Underwood, S.; Mulvaney, P. *Langmuir* **1994**, 10, 3427. (e) Nath, N.; Chilkoti, A. *Anal. Chem.* **2002**, 74, 504. (f) Oldenburg, S. J.; Averitt, R. D.; Westcott, S. L.; Halas, N. J. *Chem. Phys. Lett.* **1998**, 288, 243. (g) Henglein, A. *Langmuir* **1999**, 15, 6738. (h) Ung, T.; Liz-Marzan, L. M.; Mulvaney, P. *J. Phys. Chem. B* **2001**, 105, 3441. (i) Storhoff, J. J.; Lazarides, A. A.; Mucic, R. C.; Mirkin, C. A.; Letsinger, R. L.; Schatz, G. C. *J. Am. Chem. Soc.* **2000**, 122, 4640.

(12) (a) Henglein, A.; Meisel, D. *Langmuir* **1998**, 14, 7392. (b) Link, S.; El-sayed, M. A. *J. Phys. Chem. B* **1999**, 103, 4212. (c) Alvarez, M. M.; Khouri, J. T.; Shaaff, T. G.; Shafiqullin, M. N.; Vezmar, I.; Whetten, R. L. *J. Phys. Chem. B* **1997**, 101, 3706. (d) Heath, J. R.; Knobler, C. M.; Leff, D. V. *J. Phys. Chem. B* **1997**, 101, 189.

(13) (a) Malinsky, M. D.; Kelly, K. L.; Schatz, G. C.; Van Duyne, R. P. *J. Am. Chem. Soc.* **2001**, 123, 1471. (b) Haes, A. J.; Van Duyne, R. P. *J. Am. Chem. Soc.* **2002**, 124, 10596.

**Scheme 1. Schematic of the Overall Preparative Process of MPA-Bridged CuHCF Multilayers on the Gold Colloid Electrode**

● Stands for CuHCF

faces, the localized refractive index surrounding these nanoparticles would change, which results in absorbance increase and red-shift of native gold surface plasmon band.<sup>11</sup> The molecular adsorption and interactions can even be quantified by virtue of the sensitivity of a gold surface plasmon band to the localized environment of a nanoparticle surface.<sup>11e,13</sup> Here, when MPA-bridged CuHCF multilayers were anchored on these immobilized gold colloidal nanoparticles, obvious absorbance increase and red-shift of the surface plasmon band were observed as shown in Figure 1. The spectral changes cannot be due to the charge-transfer band in the CuHCF since CuHCF films exhibit a weak and broad absorbance band centered at about 490 nm in a reduced state and 420 nm in an oxidized state,<sup>14</sup> whereas gold nanoparticles have the strongest molar absorbance coefficient compared with the conventional molecules. This confirms qualitatively that spectral changes are due to the surrounding dielectric environmental changes coming from the anchoring of CuHCF multilayers on gold nanoparticles. Further red-shift and absorbance increase of the surface plasmon band with increasing number of layers indicate increasingly denser CuHCF shell thickness.<sup>11h,13</sup> The evenly changed spectral responses of the surface plasmon band demonstrate uniform growth of CuHCF multilayers on the immobilized nanoparticles. This kind of spectral sensitivity to particle shell thickness changes are not unexpected and has been predicted by Mie theory and demonstrated experimentally by silica-coated gold nanoparticles<sup>11h</sup> and alkanethiol self-assembled monolayers with different chain lengths on silver nanoparticles.<sup>13</sup>

The evidence from the second set of characterizations for the formation of CuHCF multilayers on the APTMS-supported nanoparticles is shown by the AFM images in Figure 2. To obtain accurate size information of immobilized nanoparticles before and after CuHCF multilayers modification, the colloid electrode with a low surface coverage of gold nanoparticles (~10% calculated by particle number counting) was constructed purposefully. (Such coverage is tunable, simply, by self-

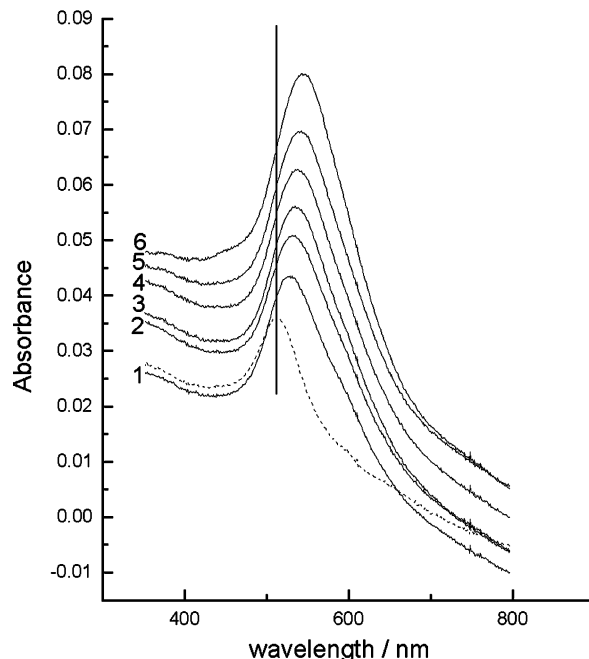


**Figure 1.** Changes of absorbance spectra for MPA-bridged CuHCF multilayers assembled on the as-prepared gold colloid electrode. Curves 1–6 correspond to 1–6 CuHCF layers, respectively. Dashed line is the absorbance spectrum of native colloid electrode.

(14) (a) Siperko, L. M. Ph.D. Thesis, Ohio State University, Columbus, OH, 1983. (b) Ellis, D.; Eckhoff, M.; Neff, V. D. *J. Phys. Chem.* **1981**, *85*, 1225. (c) Siperko, L. M.; Kuwana, T. *J. Electrochem. Soc.* **1983**, *130*, 396. (d) Itaya, K.; Akahoshi, H.; Toshima, S. *J. Electrochem. Soc.* **1982**, *129*, 1498.

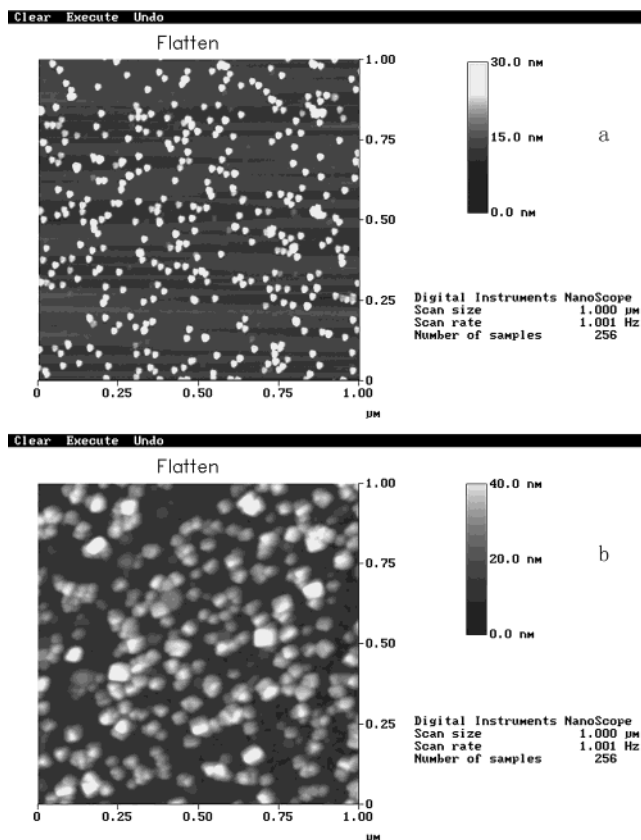


**Figure 2.** (a) Tapping mode AFM image of the colloid electrode prepared by 50-min self-assembly of APTMS-modified ITO in the as-prepared gold colloid. (b) Tapping mode AFM image of the as-prepared colloid electrode after 8-layer CuHCF anchoring; height analysis of a and b indicates selectivity of CuHCF multilayers on immobilized nanoparticles.

assembling time scale control of gold nanoparticles.<sup>1,2a</sup> Figure 2a presents the topographic image of the colloid electrode and Figure 2b is the image of the colloid electrode after 8 CuHCF multilayers anchoring following the above derivatizing procedure. Lateral dimensions are distorted due to tip convolution affects. The cross-sectional contour plots of surface topography give particle height of  $\sim 15$  nm for the immobilized gold nanoparticle and  $\sim 26$  nm for 8 CuHCF multilayers-modified gold nanoparticle. Thus, each MPA–CuHCF monolayer thickness can be estimated as  $\sim 1.38$  nm, which is in agreement with the theoretical thickness of the MPA monolayer and the unit cell dimension of a CuHCF, and also consistent with ellipsometric studies.<sup>9</sup> This demonstrates successful anchoring of CuHCF multilayers on the individual immobilized gold nanoparticles. The control experiment for APTMS-modified ITO after the above adsorption steps (8 cycles of step 3–step 5 in Scheme 1) gives only APTMS-like topography characteristics (typical overall roughness of organosilane films on glass is in the range of 1–3 nm as demonstrated by previous reports<sup>15</sup>), indicating that multilayers growth does not take place on an APTMS-exposed surface. It is concluded from these experimental facts that the MPA-bridged CuHCF multilayers grow selectively on gold nanoparticle sites and the interspaces among immobilized gold nanoparticles are still free of

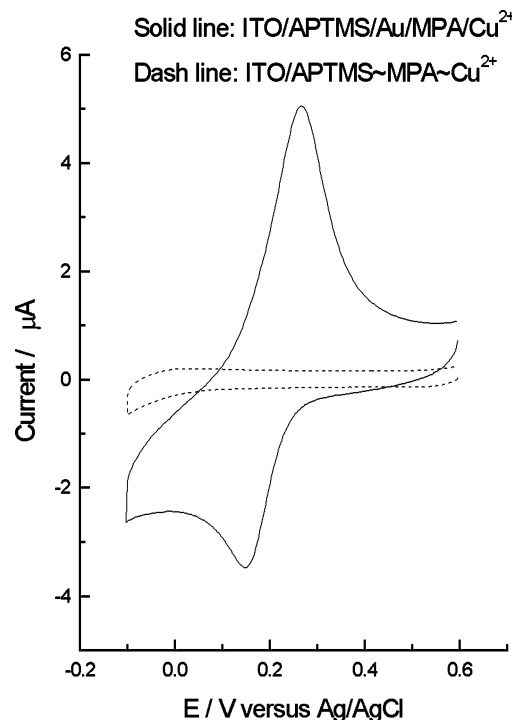


**Figure 3.** Solid line shows cyclic voltammogram of the as-prepared colloid electrode after treatments with 10 mM MPA and 10 mM CuNO<sub>3</sub>. Dashed line shows the cyclic voltammogram of APTMS-modified ITO after above-mentioned treatments. Scan rate was 50 mV/s. Supporting electrolyte: 0.1 M KNO<sub>3</sub> solution.

multilayer growth (comparison of topography characteristics for “vacant domains” in Figure 2a and Figure 2b also supports the conclusion).

The selective anchoring of MPA-bridged CuHCF multilayers on gold nanoparticle sites of the colloid electrode is also supported by electrochemistry. MPA molecules would displace physically adsorbed citrate ions and chemically adsorb on the surfaces of these immobilized nanoparticles upon immersion of the as-prepared colloid electrode into dilute MPA solution due to strong covalent binding of gold and sulfur. Subsequent immersion into aqueous solution containing Cu<sup>2+</sup> ions of MPA-modified colloid electrode results in the robust attachment of Cu<sup>2+</sup> due to effective carboxylate–copper interactions.<sup>7,9</sup> Figure 3 (solid line) shows a typical cyclic voltammogram of the as-prepared MPA–Cu<sup>2+</sup>-modified APTMS-supported colloid electrode. The oxidation peak and reduction peak are attributed to the redox process of Cu(II) and Cu(I), respectively.<sup>7c</sup> Repeated cycling only leads to a minimal loss of signal, which indicates that Cu ions remain strongly adsorbed on MPA/nanoparticles in both oxidation states. In contrast, APTMS-modified ITO after consecutive treatment with MPA and Cu(NO<sub>3</sub>)<sub>2</sub> gives only featureless responses as shown in Figure 3 (dashed line), indicating that Cu<sup>2+</sup> cannot adsorb on these sites without gold nanoparticles. This is because both Cu<sup>2+</sup> and MPA cannot interact with exposed amino groups of an APTMS surface (i.e., interspaces between immobilized gold nanoparticles). The gold nanoparticle sites-selective anchoring of MPA–Cu<sup>2+</sup> determines the selectivity of CuHCF monolayer to particle sites, which can be reproducibly prepared by treating the above MPA–Cu<sup>2+</sup>-coated colloid electrode with 10 mM potassium ferricyanide solution for 20 min.

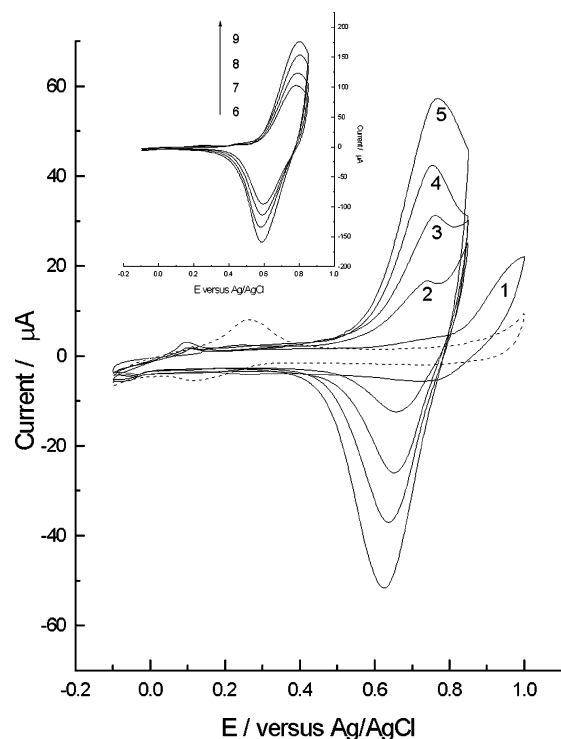


**Figure 4.** Cyclic voltammograms of the as-prepared colloid electrode with 1–9 CuHCF layers in 0.1 M KCl solution. Dashed line shows cyclic voltammogram of Cu ions adsorbed specifically to MPA-modified gold nanoparticle sites in 0.1 M KCl solution. The scan rate was 50 mV/s.

The generation of the CuHCF layer on particle surfaces results in reproducible electrochemical responses as shown in Figure 4. The redox peak with a formal potential of ca. 0.7 V is assigned to the low-spin  $\text{Fe}^{\text{II/III}}$  redox couple<sup>9</sup> in the CuHCF. The consecutive treatment (step 3–step 5 in Scheme 1) results in the generation of CuHCF multilayers-modified colloid electrode as demonstrated by linearly increasing peak currents. To test the selectivity of CuHCF multilayers to gold nanoparticle sites, we treated APTMS-modified ITO consecutively with MPA,  $\text{Cu}(\text{NO}_3)_2$ , and potassium ferricyanide; as a result, no characteristic CuHCF cyclic voltammetric responses were observed. This demonstrates selective anchoring of CuHCF multilayers on gold nanoparticle sites of the colloid electrode, which is in excellent agreement with the above optical and AFM studies.

**Comparison of Electrochemistry of CuHCF Multilayers on the Colloid Electrode and a Planar Macroelectrode.** The pioneering work of Brust et al.<sup>16</sup> demonstrated that alkanethiols form 3-D self-assembled monolayers (SAMs) on the curved surface of gold nanoparticles, which extends current interest in the study of SAMs on a planar surface<sup>17</sup> to curved nanoparticle surfaces.<sup>16</sup> As a result, attention is being focused on understanding the important similarities/differences between 2-D and 3-D SAMs. It is accepted that high

(16) Brust, M.; Walker, M.; Bethell, D.; Schiffrin, D. J.; Whyman, R. *J. Chem. Soc., Chem. Commun.* **1994**, 801.

(17) (a) Ulman, A. *An Introduction to Ultrathin Organic Films: From Langmuir Blodgett to Self-Assembled Monolayers*; Academic Press: New York, 1991, and references therein. (b) Dubois, L. H.; Nuzzo, R. G.; *Annu. Rev. Phys. Chem.* **1992**, 43, 437. (c) Chaudhari, M. K.; Whitesides, G. M. *Science* **1992**, 255, 1230.

**Table 1. Changes of fwhm and  $\Delta E_p$  with Increasing CuHCF Layer Number at 50 mV/s**

layer number	2	3	4	5	6	7	8	9	10
fwhm (mV)	145.6	150.5	162.7	167.2	169.7	179.3	183.7	184.1	184.2
$\Delta E_p$ (mV)	72.6	91.1	109.7	127.6	141.3	163.6	203.8	225.9	228.2

curvature of nanoparticle surfaces would result in great volume and hence mobility of the outmost functional groups; therefore, SAMs on gold nanoparticles sometimes show a different reactivity from their 2-D counterparts. For example, unlike 2-D SAMs,  $\omega$ -bromo-functionalized nanoparticles<sup>18</sup> have comparable  $\text{S}_{\text{N}2}$  reactivity with primary alkyl halides monomers (RBr). Also, 3-D SAMs on highly curved surfaces of gold nanoparticles are more disordered than 2-D SAMs and have a disorder approaching that of liquid alkanes,<sup>18</sup> which is supported by vibrational spectroscopy.<sup>19</sup> Sastry and co-workers demonstrate the formation of interdigitated bilayers structure on silver nanoparticle surfaces, which cannot form on a 2-D macroelectrode surface.<sup>20</sup> Andres et al. found that the gap between close-packed dodecanethiol-coated gold nanoparticles is substantially less than double length of dodecanethiol; therefore, they concluded that alkanethiols attached to adjacent nanoclusters interpenetrate the region between the nanoclusters.<sup>21</sup> Actually, the immobilized gold nanoparticles on the colloid electrode expose still curved outmost surfaces. Selective planting of MPA-bridged CuHCF multilayers on these nanoscale sites indicates that we can make a convincible contrast study of our multilayer systems associated with the colloid electrode and these on a planar macroelectrode surface.<sup>9</sup>

Table 1 shows changes of some electrochemical parameters with increasing CuHCF layers, which reveals two obvious features different from those of a planar macroelectrode: (1) a larger peak-to-peak separation and full-width at half-maximum (fwhm) than that in ref 9 (a fwhm of 92 mV in ref 9 is in close agreement with the theoretical value 90.6 mV<sup>23</sup>); (2) increasing CuHCF loading cycles result in further increase of peak-to-peak separations. It is noted that the APTMS-supported gold nanoparticles only formed submonolayers (surface coverage < 25%) due to repulsive interactions among nanoparticles.<sup>1,2</sup> Therefore, these immobilized gold nanoparticles distributed incontinuously, which results in noncontinuous distribution of CuHCF multilayers on noncontinuous nanoscale gold domains of the colloid electrode (Scheme 2), whereas CuHCF multilayer systems in ref 9 distribute continuously on uniform gold surfaces. Also, the high curved surfaces of individual immobilized nanoparticles determines the curvilinearly distributed  $\text{Fe}^{\text{II/III}}$  on nanoscale domains. These differ-

(18) Templeton, A. C.; Hostetler, M. J.; Kraft, C. T.; Murray, R. W. *J. Am. Chem. Soc.* **1998**, 120, 1906.

(19) (a) Badia, A.; Singh, S.; Demers, L.; Cuccia, L.; Brown, G. B.; Lennox, R. B. *Chem. Eur. J.* **1996**, 2, 359. (b) Badia, A.; Cuccia, L.; Demers, L.; Morin, F.; Lennox, R. B. *J. Am. Chem. Soc.* **1997**, 119, 2682. (c) Hostetler, M. J.; Stokes, J. J.; Murray, R. W. *Langmuir* **1996**, 12, 3604.

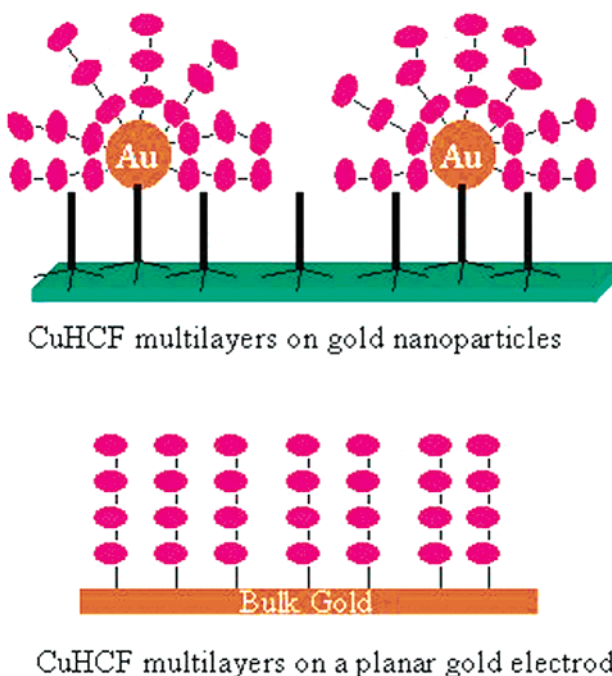
(20) Patil, V.; Mayya, K. S.; Pradhan, S. D.; Sastry, M. *J. Am. Chem. Soc.* **1997**, 119, 9281.

(21) Andres, R. P.; Bielefeld, J. D.; Henderson, J. I.; Janes, D. B.; Kolagunta, V. R.; Kubiak, C. P.; Mahoney, W. J.; Osifchin, R. G. *Science* **1996**, 273, 1690.

(22) Clark, R. A.; Bowden, E. F. *Langmuir* **1997**, 13, 559.

(23) Laviron, E. *J. Electroanal. Chem.* **1979**, 100, 263.

**Scheme 2. Schematic of Structural Difference between CuHCF Multilayers on the Colloid Electrode and Multilayers on a Planar Macroelectrode<sup>a</sup>**



<sup>a</sup> Different from multilayers on a planar macroelectrode, the multilayer growth extends three-dimensionally from a gold nanoparticle center.

ences are illustrated in Scheme 2. The various orientations and distances of redox centers to the substrate on a colloid electrode would lead to formal potential dispersions.<sup>22</sup> As a result, larger peak-to-peak separations and large fwhm were observed for these CuHCF multilayers on the colloid electrode. This kind of nonideal electrochemistry can also be observed by various scan rate experiments. For example, the colloid with 5 CuHCF layers exhibited an ill-defined linear relationship of peak current versus scan rates as shown in Figure 5. Still, the continuously increasing peak-to-peak separations with increasing CuHCF loading cycles might be due to increasing disorder of CuHCF multilayer structure (CuHCF multilayers on curved nanoscale surfaces might not be an ideally layered structure of multilayers, and increasing layer buildup would result in increasing disorder of the layer structure due to larger volume effects of outmost functional units<sup>18</sup>). The kind of disorder of CuHCF multilayers would result in additional redox potential dispersions;<sup>22</sup> as a result, increasing peak-to-peak separations were observed with increasing layer number. In short, electrochemistry of CuHCF multilayers on the colloid electrode is found to be different from that on a planar macroelectrode, which indicates that these curved surfaces of individual immobilized nanoparticles might be good electrochemical platforms for the study of molecular adsorption and interactions.

**Application Potentially.** Studies of self-assembling kinetics of gold nanoparticles on an APTMS surface demonstrated that coverage of nanoparticles on APTMS is highly tunable, simply, by self-assembling time control.<sup>1,2a</sup> This indicates that we can tune the quanti-

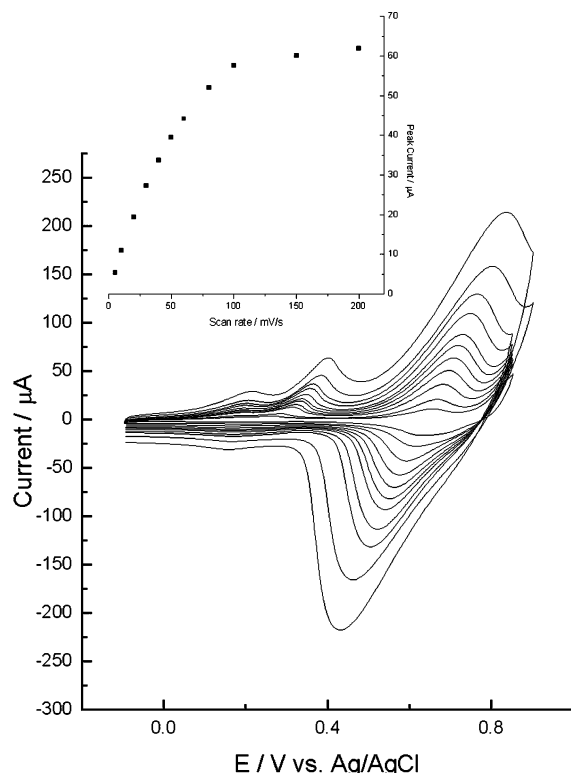


**Figure 5.** Cyclic voltammograms of the colloid electrode with 5 CuHCF layers in 0.1 M KCl solution at various scan rates: 5, 10, 20, 30, 40, 50, 60, 80, 100, 150, and 200 mV/s. Inset shows the relationship of oxidation peak current versus scan rate.

ties of CuHCF functional units by controlling both the coverage of the nanoparticles and layer numbers of the CuHCF on a solid substrate. Actually, this strategy provides higher precision in tailoring quantity and distribution of functional units than conventional self-assembled multilayer systems on a planar macroelectrode; as an additional parameter, the coverage of nanoparticles<sup>2</sup> is introduced and highly tunable by self-assembling kinetics control. This might be an advantage of the chemically modified colloid electrode, which might find sensor applications.

It is known that when functionalizing molecules adsorb on the surfaces of nanoparticles, surface charges of nanoparticles are decreased largely; as a result, van der Waals attractive forces usually drive the aggregation of these solution-state nanoparticles in solution.<sup>11</sup> Thus, anchoring complex multilayer systems to surfaces of solution-state nanoparticles is nearly unimaginable, whereas this study actually provides an alternative strategy of surface modification of gold nanoparticles: that is, to tether uncapped colloidal nanoparticles to the substrate first and then a modification procedure is done on these immobilized uncapped nanoparticles afterward. Thus, aggregation of nanoparticles in the functionalization process was averted. Also, in view of recent interest in metal hexacyanoferrates (MHCF) as potential molecular magnets,<sup>24</sup> incorporating CuHCF multilayers into high-area-ratio surfaces of nanoparticles has significance in future nanoelectronic applications. We accomplished functionalization of gold nanoparticles

with tiny molecular magnets (CuHCF multilayers) by tethering of these uncapped nanoparticles to a solid substrate and postmodification. Actually, this strategy solves simultaneously the immobilization and functionalization of nanoparticles on a solid substrate and awaits direct nanoelectronic device applications.

### Conclusions

Self-assembled MPA-bridged CuHCF multilayers on a planar macroelectrode<sup>9</sup> were copied safely to the as-prepared APTMS-supported colloid electrode. Highly selective anchoring of CuHCF multilayers on these immobilized gold nanoparticles of the colloid electrode was demonstrated. The CuHCF multilayers associated with the colloid electrode are distributed three-dimensionally in nanoscale dimensions; as a result, redox potential dispersions result in nonideal surface-confined

electrochemistry. It follows that curved surfaces of individual immobilized nanoparticles might be good platforms for studies of conventional molecular adsorptive phenomena, simply, by coping similar experimental procedures on a macroelectrode to the colloid electrode. One obvious advantage is that this adsorptive process can be accurately monitored by metal surface plasmon spectroscopy. Also, reports of monolayers,<sup>3–4</sup> multilayers, and UPD<sup>5</sup> atom layers on a colloid electrode indicate that surfaces of immobilized nanoparticles are also excellent templates for synthesis of surface-confined nanomaterials.

**Acknowledgment.** This work was supported by the National Science Foundation of China. (No. 20275037, No. 29975028).

CM021052L